Determination of bridge lifetime dynamic amplification factor using finite element analysis of critical loading scenarios

Arturo González , Paraic Rattigan, Eugene J. OBrien and Colin Caprani

Abstract

The development of accurate codes for the design of bridges and the evaluation of existing structures requires adequate assessment of heavy traffic loading and also the dynamic interaction that may occur as this traffic traverses the structure. Current approaches generally first calculate characteristic static load effect and then apply an amplification factor to allow for dynamics. This neglects the significantly-reduced probability of both high static loading and high dynamic amplification occurring simultaneously. This paper presents an assessment procedure whereby only critical loading events are considered to allow for an efficient and accurate determination of independent values for characteristic (lifetime-maximum) static and total (including dynamic interaction) load effects. Initially the critical static loading scenarios for a chosen bridge are determined from Monte Carlo simulation using weigh-in-motion data. The development of a database of 3-dimensional finite element bridge and truck models allows for the analysis of these various combinations of vehicular loading patterns. The identified critical loading scenarios are modelled and analysed individually to obtain the critical total load effect. It is then possible to obtain a correlation between critical static load effect and corresponding total load effect and to extrapolate to find a site-specific dynamic amplification factor.

1. Introduction

Correct evaluation of the behaviour of highway bridges under heavy loading is extremely important both for the enhancement of design techniques, and for the assessment of existing infrastructure. It is widely accepted that codes for the design of new bridges are highly conservative in their allowance for dynamics which is appropriate given the small marginal cost of increasing capacity in most cases, but such conservatism is inappropriate for the assessment of highway bridges [1,2].

In the case of short/medium span bridges (20 - 30 m), the critical traffic loading event typically consists of two heavy trucks meeting or passing on the bridge. These critical events are commonly obtained using Monte Carlo simulation in tandem with measured Weigh in Motion (WIM) data [3,4,5]. Once the worst static case is known, the final traffic load is commonly calculated through the application of a Dynamic Amplification Factor (DAF), that accounts for the dynamic component contained in the bridge response [6,7,8]. DAF is defined as the ratio of maximum total load effect to maximum static load effect for a given loading event (combination of trucks crossing).

It is known that dynamic interaction is influenced by numerous bridge- and vehicle-dependent dynamic parameters, such as vehicle velocity, road profile, suspension and tyre stiffness [9,10,11]. The dynamic amplification factors prescribed in design/assessment codes are sometimes based on dynamic load tests of existing bridges and tend to be conservative. There is considerably discrepancy among the values recommended by different codes due to the complexity of the vehicle bridge interaction problem. They typically suggest a dynamic amplification which is function only of a few general parameters (i.e., bridge length or natural frequency, number of lanes and

load effect) that ignore many of these significant bridge and truck dynamic characteristics. As part of the SAMARIS project [12], experiments took place on a medium-span bridge showing evidence that the dynamic amplification decreases as the gross vehicle weight increases and also that the dynamic load factors for two truck loading events are less than for one truck loading events.

Complex dynamic bridge truck interaction models have been developed, using finite element packages, to aid understanding of the interaction that can be expected in vehicle crossing events [1,13-16]. This paper uses a finite element analysis approach to assess the levels of dynamic interaction occurring for the statistically obtained critical loading scenarios of a beam-and-slab bridge. A procedure is described by which a site-specific allowance for dynamics can be found. This dynamic allowance can be extrapolated to the 100-year bridge lifetime using multivariate extreme value analysis [4].

2. Description of vehicle bridge interaction finite element models

An elaborate vehicle bridge interaction model is necessary to allow for 3-dimensional aspects, such as the transverse effect of multiple vehicles, that have a significant influence on the total response and simpler models can not capture.

2.1 Vehicle bridge interaction modelling

The authors use MSc/NASTRAN [17] and a Lagrange technique to model the load imposed by a truck crossing a bridge. The Lagrange multiplier formulation allows

for the representation of the compatibility condition at the bridge/vehicle interface through a set of auxiliary functions. Cifuentes [18] uses this formulation to solve for the motion of a single circular mass moving at constant speed on a one-dimensional bridge model. This approach can be extended to allow for the presence of multiple masses travelling in given paths at different speeds [15]. The bridge structure along any travel path is divided into (N-1) finite elements, with coordinates $x_1, x_2, \ldots x_N$ adopted for the N nodes. The variables defining the behaviour of the bridge are:

$z(x,t)$: vertical deflection of the bridge in position x at time t,

$z_i = z_i(t)$: deflection of node i at time t,

$\theta_i = \theta_i(t)$: rotation of node i at time t,

$\ddot{z}_i = \ddot{z}_i(t)$: acceleration of vertical displacement in node i at time t,

$\ddot{\theta}_i = \ddot{\theta}_i(t)$: acceleration of rotation in node i at time t.

The variables defining the behaviour of a series of moving masses j (one per wheel or one per axle in a 3D or 2D problem respectively) are:

$v_j = v_j(t)$: time-dependent velocity of the vehicle. If there are different vehicles, v_j might be different for each vehicle.

m_j : mass of wheel j,

$w_j = w_j(t) = z(\zeta_j, t)$: vertical displacement of wheel j measured with respect to the horizontal axis,

$R_j = R_j(t)$: Interaction force at contact point of wheel j,

$\zeta_j = \zeta_j(t)$: Distance x travelled on the bridge by moving wheel j at time t.

The variable ζ_j denoting position of mass j on the bridge at time t can be defined as a function of the velocity input $v_j(t)$ as:

$$\zeta_j = \int_{t_j}^{t} v_j(t)dt = \sum_{t=t_j}^{t} v_j(t)\Delta t \qquad 0 \le \zeta_j \le L \tag{1}$$

where time t_j is the instant at which mass j enters the bridge and L is the bridge length.

For an undamped model, the equation of motion of the bridge finite element model can be written as:

$$\begin{bmatrix} m_{11} & m_{12} & . & . & . \\ m_{21} & m_{22} & . & . & . \\ . & . & . & . & . \\ . & . & . & m_{2N-1,2N-1} & m_{2N-1,2N} \\ . & . & . & m_{2N,2N-1} & m_{2N,2N} \end{bmatrix} \begin{Bmatrix} \ddot{z}_1 \\ \ddot{\theta}_1 \\ . \\ \ddot{z}_N \\ \ddot{\theta}_N \end{Bmatrix} + \begin{bmatrix} k_{11} & k_{12} & . & . & . \\ k_{21} & k_{22} & . & . & . \\ . & . & . & . & . \\ . & . & . & k_{2N-1,2N-1} & k_{2N-1,2N} \\ . & . & . & k_{2N,2N-1} & k_{2N,2N} \end{bmatrix} \begin{Bmatrix} z_1 \\ \theta_1 \\ . \\ z_N \\ \theta_N \end{Bmatrix} = \begin{Bmatrix} f_1 \\ M_1 \\ . \\ f_N \\ M_N \end{Bmatrix} \tag{2}$$

where $[m_{ij}]_{2Nx2N}$ is the mass matrix of the finite element model and $[k_{ij}]_{2Nx2N}$ is the stiffness matrix, representing the dynamic characteristics of the bridge model. $\{z_i\}_{2Nx1}$ is a vector containing displacements (z_i) and rotation (θ_i) of the nodes, and $\{\ddot{z}_i\}_{2Nx1}$ their acceleration at time t. In the right-hand side of the equation, vector $\{f\}_{2Nx1}$ represents the forces $f_i(t)$ and moments $M_i(t)$ acting on each node i at a time t due to the moving loads.

A compatibility condition between the vertical displacement $w_j(t)$ of each mass j and the bridge at the contact point must be established at any time t. For this purpose, a set of auxiliary functions $A_{ij}(t)$ and $B_{ij}(t)$ are defined for every mass j, and the compatibility condition at the contact point of mass j is formulated as [18]:

$$w_j(t) = \sum_{i=1}^{N} A_{ij}(t) z_i(t) + \sum_{i=1}^{N} B_{ij}(t) \theta_i(t) \qquad ; \quad j=1,2, \ldots p \tag{3}$$

where $z_i(t)$ and $\theta_i(t)$ are the displacement and rotation at each node i, N is the total number of bridge nodes, p *is* total number of moving loads, and $A_{ij}(t)$ and $B_{ij}(t)$ are the auxiliary functions for load j. $A_{ij}(t)$ and $B_{ij}(t)$ can adopt different values in each node i at each instant t.

The shape of these auxiliary functions is shown in Fig. 1. The functions have zero value out of the interval between adjacent nodes. $A_{ij}(t)$ and $B_{ij}(t)$ are completely defined once $v_j(t)$, approach length, axle spacings and the coordinates of the bridge nodes are known. Each axle takes a different time to reach the same node and each wheel of the same axle follows a different path on the bridge. Thus, the auxiliary functions are different for each mass j , and for each time t.

According to Cifuentes [18], the interaction force, $R_j(t)$, between a moving circular mass m_j and the bridge structure, is composed of the inertial force due to vertical motion of the mass ($-m_j \left[\frac{\partial^2 z(x,t)}{\partial t^2} \right]_{(\xi_j,t)}$), the Coriolis force due to relative motion between the bridge and the load ($-2m_j v_j \left[\frac{\partial^2 z(x,t)}{\partial x \partial t} \right]_{(\xi_j,t)}$), the centripetal force due to circular motion following the deformed shape of the bridge acting towards the centre of the mass ($-m_j v_j^{\,2} \left[\frac{\partial^2 z(x,t)}{\partial x^2} \right]_{(\xi_j,t)}$), and the weight due to gravity force ($-m_j g$).

Hence the interaction force can be defined as:

$$R_j = -m_j\{\ddot{z} + 2v_j\dot{z}' + v_j{}^2 z'' + g\}\delta(x-\xi_j) \tag{4}$$

where $\ddot{z} = \left[\frac{\partial^2 z(x,t)}{\partial t^2}\right]_{(\xi_j,t)}$, $\dot{z}' = \left[\frac{\partial^2 z(x,t)}{\partial x \partial t}\right]_{(\xi_j,t)}$, $z'' = \left[\frac{\partial^2 z(x,t)}{\partial x^2}\right]_{(\xi_j,t)}$ and δ is the Dirac function. If $x \neq \zeta_j, R_j = 0$, where ζ_j is the distance travelled by the mass *j* as defined in Eq. (1).

By combining Eqs. (3) and (4), the interaction force, R_j, between the bridge and the j^{th} mass can also be expressed as:

$$R_j = -m_j\ddot{w}_j - m_j g - m_j[2v_j\dot{z}' + v_j{}^2 z''] \tag{5}$$

Using the Lagrange multiplier functions and re-ordering terms:

$$m_j\ddot{w}_j + R_j = -m_j g - m_j\sum_i A_i[2v_{ij}\dot{z}_i' + v_{ij}{}^2 z_i''] \tag{6}$$

where $v_{ij} = v_j(t_i)$, that is, velocity of mass m_j when it reaches node *i*.

The roughness of the pavement surface *r(x)* can be imported into Equation (6) by taking into account that vertical displacement of the mass m_j will be equal to the vertical deformation of the beam minus the depth of the irregularities at the same location. This gives:

$$m_j\ddot{w} + R_j = -m_j g - m_j\sum_i A_i[2v_{ij}\dot{z}_i' + v_{ij}{}^2 z_i'' + v_{ij}{}^2 r_i''] \tag{7}$$

An initial deflected shape of the bridge can be introduced in the same way. Therefore, the total force $f_i(t)$ and moment $M_i(t)$ acting on a bridge node i at time t due to p different masses can be expressed using the auxiliary functions as:

$$\begin{Bmatrix} f_1 \\ M_1 \\ f_2 \\ M_2 \\ . \\ . \\ f_N \\ M_N \end{Bmatrix} = \begin{Bmatrix} A_{11} \\ B_{11} \\ A_{21} \\ B_{21} \\ . \\ . \\ A_{N1} \\ B_{N1} \end{Bmatrix} R_1 + \ldots + \begin{Bmatrix} A_{1p} \\ B_{1p} \\ A_{2p} \\ B_{2p} \\ . \\ . \\ A_{Np} \\ B_{Np} \end{Bmatrix} R_p \tag{8}$$

Finally, the equations of motion of the complete moving load plus finite element model are given by:

$$[S] \begin{Bmatrix} z_1 \\ \theta_1 \\ \ldots \\ z_N \\ \theta_N \\ w_1 \\ R_1 \\ \ldots \\ w_p \\ R_p \end{Bmatrix} = \begin{Bmatrix} \sum_{j=1}^{r} A_{1j} R_j \\ \sum_{j=1}^{r} B_{1j} R_j \\ \ldots \\ \sum_{j=1}^{r} A_{Nj} R_j \\ \sum_{j=1}^{r} B_{Nj} R_j \\ -m_1 g + c_1 \\ \sum_{i=1}^{N} [A_{i1} z_i + B_{i1} \theta_i] \\ \ldots \\ -m_p g + c_p \\ \sum_{i=1}^{N} [A_{ip} z_i + B_{ip} \theta_i] \end{Bmatrix} \tag{9}$$

where

$$[S]=\begin{bmatrix}
m_{11}\frac{\partial^2}{\partial t}+k_{11} & m_{12}\frac{\partial^2}{\partial t}+k_{12} & \dots & \dots & 0 & 0 & 0 & \dots & 0 & 0 \\
m_{21}\frac{\partial^2}{\partial t}+k_{21} & m_{22}\frac{\partial^2}{\partial t}+k_{22} & \dots & \dots & 0 & 0 & 0 & \dots & 0 & 0 \\
\dots & \dots & \dots & \dots & \dots & \dots & \dots & \dots & \dots & \dots \\
\dots & \dots & \dots & m_{2N-1,2N-1}\frac{\partial^2}{\partial t}+k_{2N-1,2N-1} & m_{2N-1,2N}\frac{\partial^2}{\partial t}+k_{2N-1,2N} & 0 & 0 & \dots & 0 & 0 \\
\dots & \dots & \dots & m_{2N,2N-1}\frac{\partial^2}{\partial t}+k_{2N,2N-1} & m_{2N,2N}\frac{\partial^2}{\partial t}+k_{2N,2N} & 0 & 0 & \dots & 0 & 0 \\
0 & 0 & \dots & 0 & 0 & m_1\frac{\partial^2}{\partial t} & 1 & \dots & 0 & 0 \\
0 & 0 & \dots & 0 & 0 & 1 & 0 & \dots & 0 & 0 \\
\dots & \dots & \dots & \dots & \dots & \dots & \dots & \dots & \dots & \dots \\
0 & 0 & \dots & 0 & 0 & 0 & 0 & \dots & m_p\frac{\partial^2}{\partial t} & 1 \\
0 & 0 & \dots & 0 & 0 & 0 & 0 & \dots & 1 & 0
\end{bmatrix} \tag{10}$$

The last (*2p*) rows in Eq. (9) represent the equations of motion of each moving mass and the compatibility condition between deflections of the moving masses and the bridge. In these last rows of the global load vector, the parameter c_j is given by:

$$c_j=-\sum_{i=1}^{N}\frac{2v_{ij}m_j}{x_i-x_{i-1}}\dot{z}_{ij}A_{ij}+\sum_{i=1}^{N}\frac{2v_{ij}m_j}{x_i-x_{i-1}}\dot{z}_{i-1j}A_{ij}+\sum_{i=1}^{N}\frac{v_{ij}{}^2m_j}{x_i-x_{i-1}}\theta_{ij}A_{ij}+\sum_{i=1}^{N}\frac{v_{ij}{}^2m_j}{x_i-x_{i-1}}\theta_{i-1j}A_{ij} \qquad j=1,\dots,p \tag{11}$$

When the dynamic simulation of a truck travelling over a bridge is carried out in the following section, this term *c* is ignored. Also, the centripetal and Coriolis forces are not taken into account as most of the vehicle mass (except wheel mass) is not under circular motion and the vehicle speeds are relatively small.

2.2 Bridge and truck finite element models

The bridge chosen for this study is the Mura River Bridge in Slovenia. The bridge is 32m long and has two lanes of bi-directional traffic flow. The bridge, of beam and slab construction, is simply supported and forms part of a larger structure. Five concrete longitudinal beams support a concrete slab, with a layer of asphalt acting as the road surface. Five concrete diaphragm beams are also present in the transverse direction. The bridge has been previously modelled, instrumented and validated [19] and it is modelled using beam and plate elements as shown in Fig. 2. The vibrational mode shapes of the model are consistent with experimental results (first natural longitudinal frequency of 3.5 Hz, first torsional frequency of 4.6 Hz, and damping 3%).

The finite element truck models are modelled using rigid bodies supported by suspension and tyre systems. The body mass in the trucks is distributed uniformly throughout the frame in addition to mass elements representing the cabin and cargo masses rigidly connected to the frame. The 5-axle and 4-axle vehicle models allow for articulation between the tractor and trailer. The 3-axle and 2-axle vehicle models are rigid bodied. The suspensions and tyres are modelled as standard spring dashpot systems, taking typical stiffness and damping values from literature [14,15]. Fig. 3 shows two typical modes of vibration for the NASTRAN model of the 5-axle truck trucks. Body and axle hop frequencies vary with laden weight but they generally fall in the ranges [1.5-4.5 Hz] and [8-16 Hz] respectively.

A smooth road profile (Class ‘A’ according to the ISO standard [20]) is used to excite dynamics, and a section of this profile is presented in Fig. 4.

3. Calculation of critical static loading events

3.1 Simulation set-up

In order to conduct Monte Carlo simulation of a great number of static load cases for the bridge it is necessary obtain from the NASTRAN bridge model the static response to an axle of unit weight at any point on the travel path. The load effect of interest is taken to be midspan stress. Therefore, the influence lines of midspan stress, for each of the 5 longitudinal beams, for both of the lane loading possibilities are obtained from the FE model. It is noted that the longitudinal beams are not symmetrical about the bridge centre line, and as a result the influence lines for both allowable lane loadings must be obtained. Continental European driving laws are applicable (driving on right). Consequently the wheel paths for trucks in either lane are at 840 mm and 2660 mm from bridge centre-line for driver and passenger sides respectively. A schematic layout of the bridge is shown in Fig. 5.

The influence lines for each lane loading are obtained by placing a static load of 5 kN on each of the wheel paths for the respective lane. This is equivalent to a static axle load of 10 kN being applied by a particular truck axle. The loads are moved at 1m increments in the direction of traffic flow to obtain the influence lines of beam stress at midspan as shown in Figs. 6(a) and (b) for load directions D1 and D2 respectively.

The obtained influence lines are then normalised to give the response due to a unit axle load. Piece-wise polynomial equations are used to algebraically model the influence lines obtained. These can be used to rapidly calculate bridge static response due to random traffic flow. Eq. (12) gives the superposition equation.

$$\varepsilon_{static}(t) = \sum_{j=1}^{M} \sum_{i=1}^{N_j} W_{ij} I(x_{ij}(t)) \tag{12}$$

where $\varepsilon_{static}(t)$ is the static load effect at time t, M is the number of trucks, N_j is the number of axles in truck j, $x_{ij}(t)$ is the position on the bridge of axle i in truck j at instant t, $I(x_{ij})$ is the influence line ordinate at the specified location x_{ij} at instant t, and W_{ij} is the static weight of axle i in truck j.

3.2 Statistical calculation of critical loading events

One week of WIM data was taken from the A6 motorway near Auxerre, France. The site has 4 lanes of traffic (2 in each direction) but only the traffic recorded in the slow lanes was used and it is acknowledged that this results in conservative loading. In total 17756 and 18617 trucks were measured in the north and south slow lanes respectively, with an average daily truck flow of 6744 trucks [4]. Statistical distributions were fit to the traffic characteristics of the site for each lane.

The load effect chosen for analysis is the maximum midspan stress in longitudinal beam 1 (Fig. 5). Monte Carlo simulation is applied, using the fitted distributions to generate 10 years of bi-directional, free-flowing traffic data. This traffic is passed over the influence line for beam 1 to determine the static load effects that result. In the case of medium span bridges (< 40 m), the critical traffic event typically consists of two heavy trucks crossing the bridge at the same time. However, all possible configurations of vehicles and vehicle meeting events were considered, and some of the worst cases consisted of 3-truck event crossings involving 2 trucks in the same lane over beam 1.

Each year of simulated traffic consists of 10 representative periods, loosely termed months, of 25 working days each (allowing for 52 weekends and 11 public

holidays per annum). The events corresponding to monthly-maximum static load effect are retained, for each 'month' in each of the 10 years of flow. This is done to minimize the number of events that are to be dynamically analysed, as well as providing a shorter 'extrapolation distance'. Thus there are 100 critical events corresponding to the 100 monthly maxima, retained for dynamic analysis. The data retained for a typical critical event is presented in Table 1 (this event consists of the meeting of a 5-axle vehicle in lane D1 with a 4-axle vehicle in Lane D2).

Of the 100 monthly-maximum events, 20 are found to be one-truck events, 77 to be two-truck events and 3 are three-truck events. The influence surface for beam 1 is asymmetrical (Fig. 6); therefore trucks in lane D1 dominate, reducing the effect of trucks in lane D2. Hence the monthly-maximum events are derived from the occurrence of heavy trucks in lane D1, and trucks with less extreme gross weight in lane D2, as can be seen in Table 1.

3.3 Dynamic analysis of worst monthly loading cases

Each of the 100 cases is individually modelled and simulated using MSc/NASTRAN and the FE models described in Section 2. An entry is generated in the assembled stiffness matrix of the vehicle-bridge NASTRAN finite element system as shown in Eq. (9), and the interaction forces F_j at the contact point of each wheel j on the bridge are defined as in Eq. (8) through a bulk data file. From the generated responses it is possible to obtain the maximum total load effect in beam 1, for each individual loading event. The length of the approach is modified to ensure that vehicles meet at the prescribed location in the monthly-maximum static load case. A minimum approach

length of 100m is specified to ensure the dynamic models have achieved a suitable level of stability before crossing the bridge. Figs. 7(a) and (b) illustrate some examples of the monthly-maximum events and the corresponding total stress at midspan; the prevalence of heavy trucks in lane D1 (top lane) is again evident.

4. Determination of site-specific dynamic amplification factor

The static and total stress results from the FE simulations of the 100 events are presented in Fig. 8, which illustrates the scatter in the results. A best fit line through the data corresponds to a ratio of total to static of about 1.05. This best fit is approximately parallel to the best fit line through the static maxima. In Fig. 9, the results are ranked by monthly-maximum static stress. The static response is approximately linear while the total response is more variable. Bridge DAF is also plotted in the figure.

The Eurocode working group recommends a DAF value of 1.17 for a bridge length of 32 m and 2 lanes [6], but even though it is apparent that DAF values of magnitude 1.2 to 1.5 may be obtained for the chosen bridge and light trucks [16,19], these high order DAF values are not evident in the analysis of the bridge's critical loading events. For example, within these 100 critical loading events, the mean DAF is 1.035 with a standard deviation of 0.041. The ratio of the maximum total response to the maximum static response over this 10-year sample period is 1.06, which in this case corresponds to the same traffic event. Therefore, the 100th worst static load effect is 22% less than the load effect due to the heaviest statically weighed truck. This means that a static loading case below the 100th would require a DAF well in excess of 1.3 (=1.22*1.06) to cause higher strain than the derived maximum stress.

5. Conclusions

In this paper, the current means of allowing for dynamic interaction of bridge and truck(s) have been reviewed for a particular bridge specific and specific traffic conditions. Monte Carlo simulation of static load effect has been used to obtain monthly maximum loading events, which are then modelled and analysed dynamically using NASTRAN to obtain the total load effect. It has been shown that by individually assessing the dynamic response due to critical loading a more bridge specific value of DAF can be obtained. The procedure has been demonstrated for an existing beam-and-slab bridge with a very good road profile subject to traffic from a typical European route. Simulation results have shown that the dynamic amplification factor may result lower than the value proposed by design codes and that accurate dynamic finite element modelling can lead to significant savings in structural assessment.

Acknowledgements

The authors wish to acknowledge the continued financial assistance provided by the Irish Research Council for Science, Engineering and Technology (Embark Initiative).

References

[1] Gonzalez A, O'Connor AJ, OBrien EJ. An assessment of the influence of dynamic interaction modeling on predicted characteristic load effects in bridges. Proceedings of the 3rd International Conference on Current and Future Trends in Bridge Design, Construction and Maintenance, Shanghai, China; 2003, 241-249.

[2] DIVINE Programme, OECD. Dynamic interaction of heavy vehicles with roads and bridges. DIVINE Concluding Conference, Ottawa, Canada, 1997.

[3] O'Connor AJ, OBrien EJ. Traffic load modeling and factors influencing the accuracy of predicted extremes. Canadian Journal of Civil Engineering 2005;32:270-278.

[4] Caprani C. Probabilistic analysis of highway bridge traffic loading. PhD Thesis, UCD School of Architecture, Landscape and Civil Engineering, University College Dublin, Dublin, Ireland, 2005.

[5] Nowak AS, Hong YK. Bridge live load models. ASCE Journal of Structural Engineering 1991;117(9):2757-2767.

[6] Dawe P. Traffic loading on highway bridges. Thomas Telford, London, 2003.

[7] Chaterjee S. The design of modern steel bridges. Oxford BSP Professional Books, 1991.

[8] Zhang Q-L, Vrouwenvelder A, Wardenier J. Dynamic amplification factors and EUDL of bridges under random traffic flows. Journal of Engineering Structures 2000; 23:663-672.

[9] Green MF, Cebon D. Dynamic interaction between heavy vehicles and highway bridges. Computers and Structures 1995; 62(2):253-264.

[10] Brady SP, OBrien EJ. The effect of vehicle velocity on the dynamic amplification of two vehicles crossing a simply supported bridge. ASCE Journal of Bridge Engineering 2006; 11(2) :250-256.

[11] OBrien EJ, Li Y, González A. Bridge roughness index as an indicator of bridge dynamic amplification. Computers and Structures 2006; 84:759-769.

[12] SAMARIS Programme. Guidance for the optimal assessment of highway structures. Sustainable and Advanced Materials for Road Infrastructure, Deliverable SAM-GE-D30, EU 6th framework, 2006.

[13] Kwasniewski L Li H, Wekezer J, Malachowski J. Finite element analysis of vehicle-bridge interaction. Finite Elements in Analysis and Design 2006; 42(11):950-959.

[14] Kirkegaard PH, Nielson SRK, Enevoldson I. Heavy vehicles on minor highway bridges – dynamic modeling of vehicles and bridges, Department of Building Technology and Structural Engineering, Aalborg University, ISSN 1395-7953 R9721, 1997.

[15] Baumgärtner W. Bridge-vehicle interaction using extended FE analysis. Heavy Vehicle Systems, Int. Journal of Vehicle Design 1999; 6(1-4):1–12.

[16] Rattigan P, González A, OBrien E, Brady SP. Transverse variation of dynamic effects on beam-and-slab medium span bridges. Proceedings of the 6th International Conference on Structural Dynamics, EURODYN 2005, C.Soize & G.I. Schuëller (eds), Paris, France, 4-7 September; 2005, 1643-1649.

[17] MSC/NASTRAN for Windows. Advanced dynamic analysis user's guide version 70. The MacNeal-Schwendler Corporation, USA, 1997.

[18] Cifuentes AO. Dynamic response of a beam excited by a moving mass. Finite Elements in Analysis and Design 5, Elsevier Science Publishers B.V., Amsterdam, The Netherlands; 1989, 237-246.

[19] Brady SP, OBrien EJ, Žnidarič A. The effect of vehicle velocity on the dynamic amplification of a vehicle crossing a simply supported bridge. ASCE Journal of Bridge Engineering 2006; 11(2):241-249.

[20] ISO 8608:1995. Mechanical vibration-road surface profiles-reporting of measure data, 1995.

Table 1 Typical two-truck meeting event data file.

Lane	Axle Weights (kg/100)					Axle Spacings (m)				Velocity (m/s)	Approach (m)
	W1	W2	W3	W4	W5	AS1	AS2	AS3	AS4		
D2	49	80.4	46.1	46.1	-	3	5.7	1.3	-	20.2	100
D1	92.2	198.1	148.1	148.1	148.1	3.5	5.1	1.1	1.1	24.7	128.5

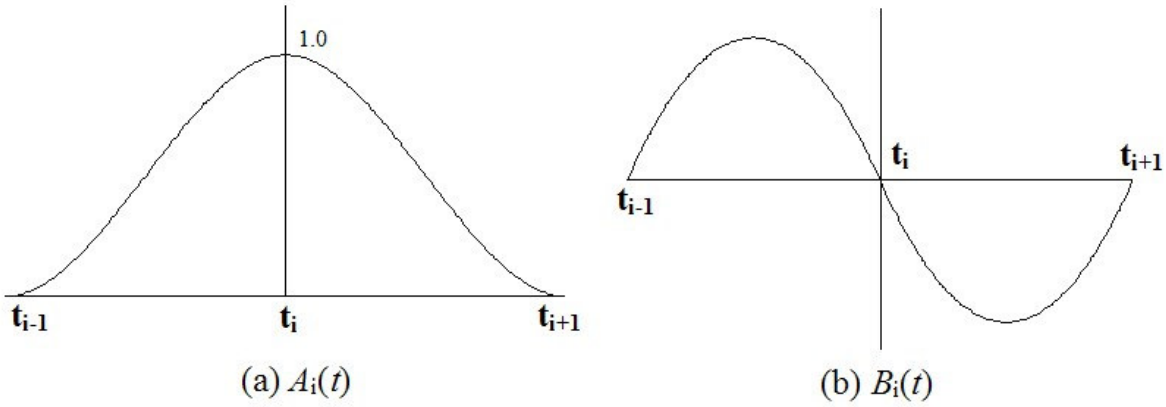

Figure 1 Auxiliary functions.

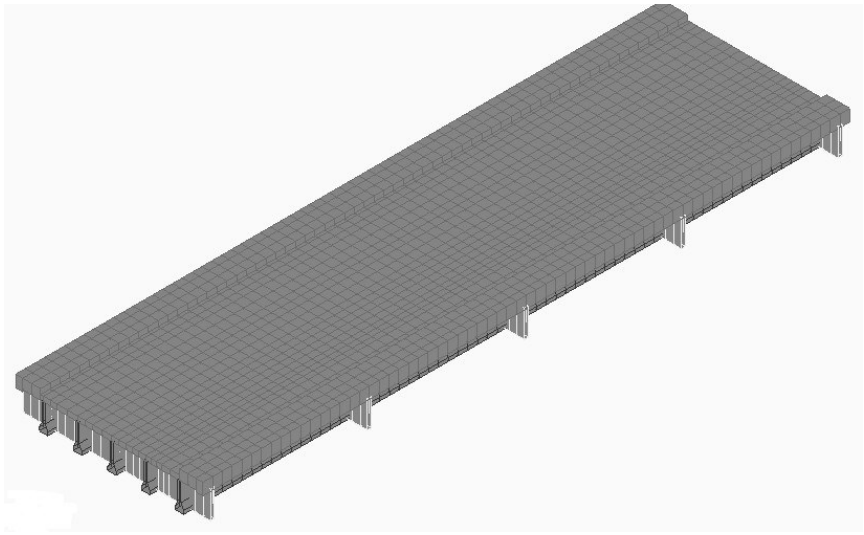

Figure 2 Bridge model.

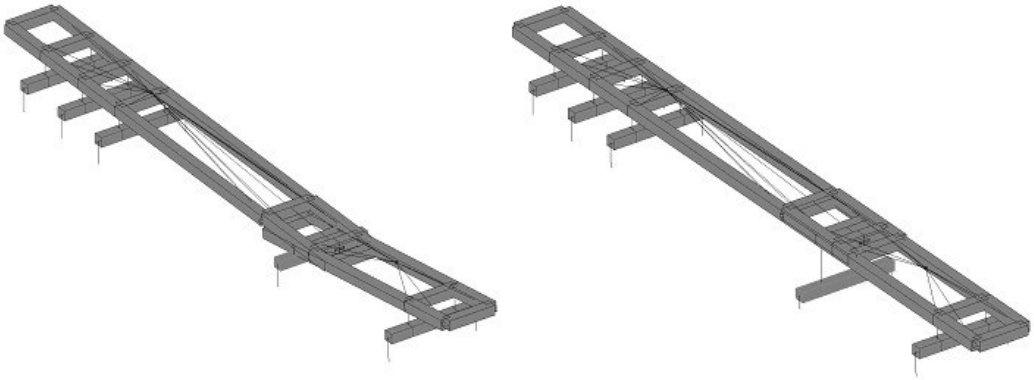

(a) Body pitch (b) 2nd axle hop

Figure 3 Truck model.

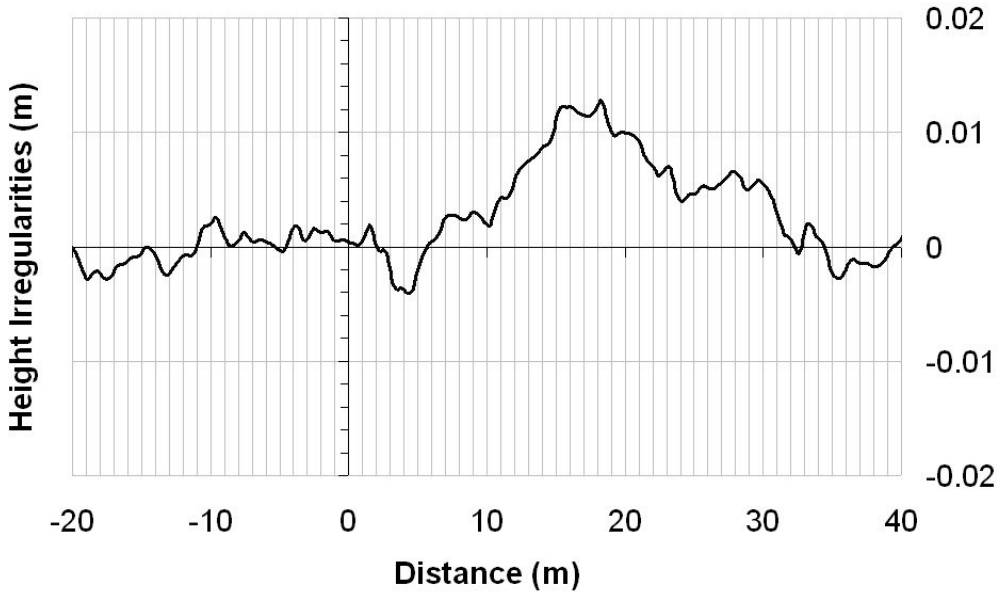

Figure 4 Road surface profile.

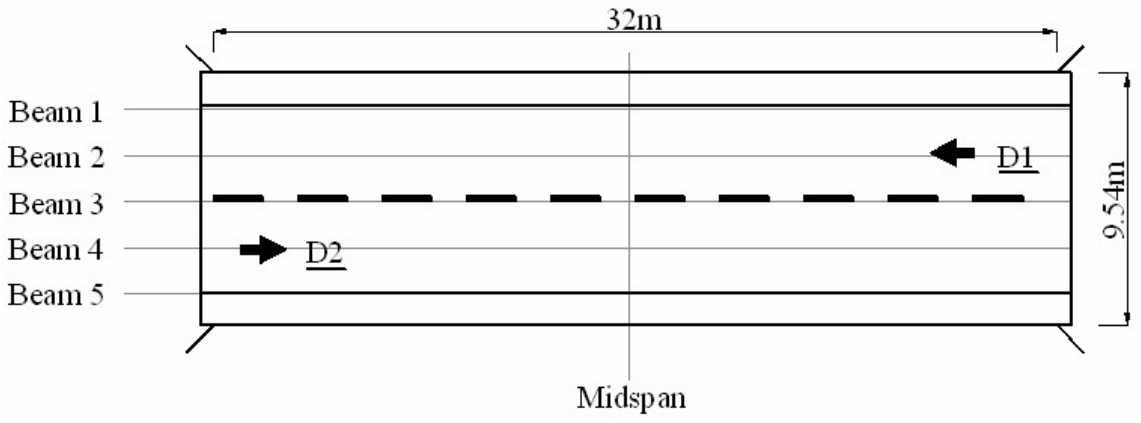

Figure 5 Schematic of bridge showing beam layout.

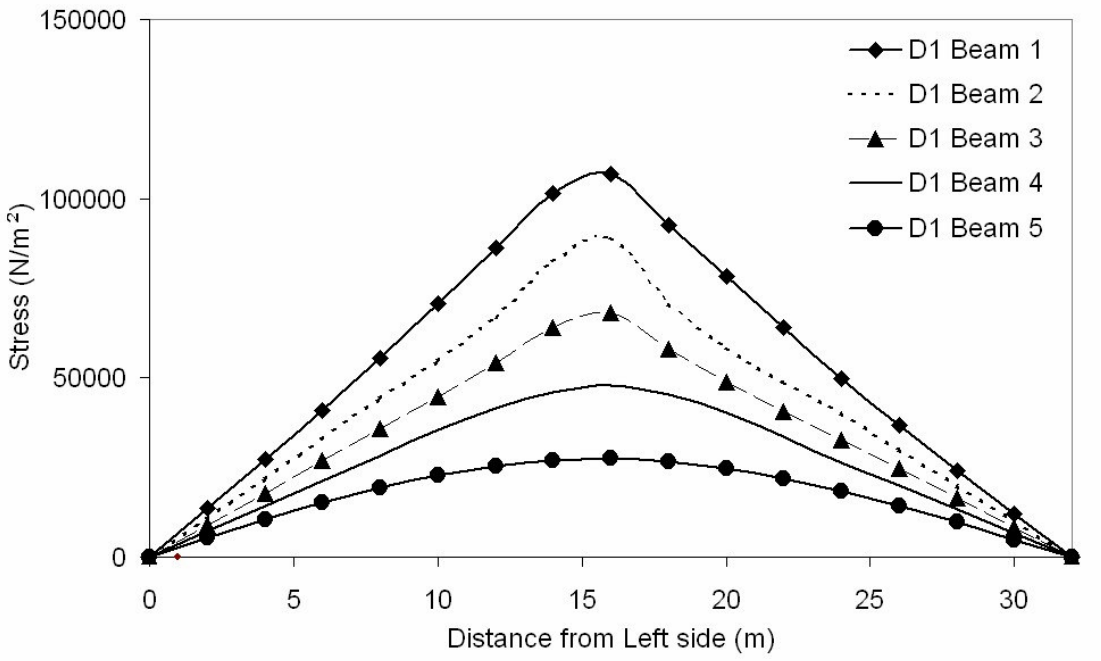

Figure 6(a) Midspan influence lines due to load moving in lane D1.

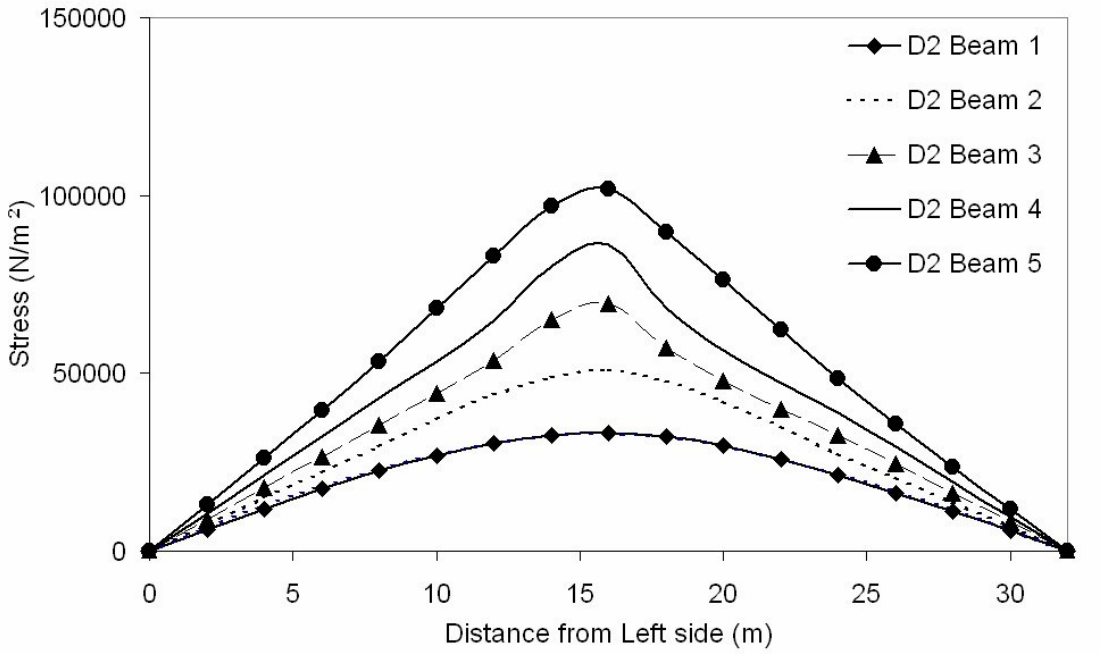

Figure 6(b) Midspan influence lines due to load moving in lane D2.

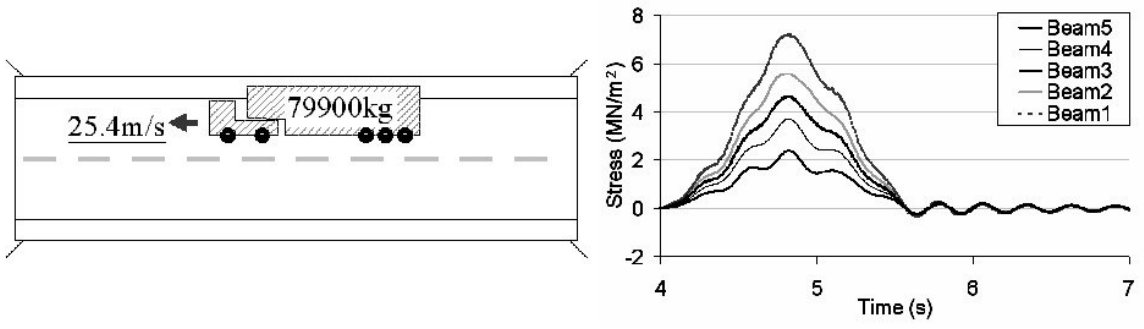

Figure 7(a) Example of one-truck crossing monthly maximum event.

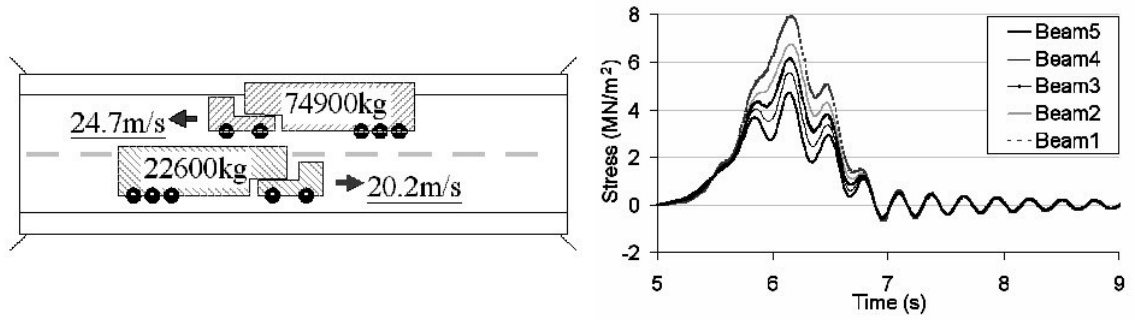

Figure 7(b) Example of two-truck crossing monthly maximum event.

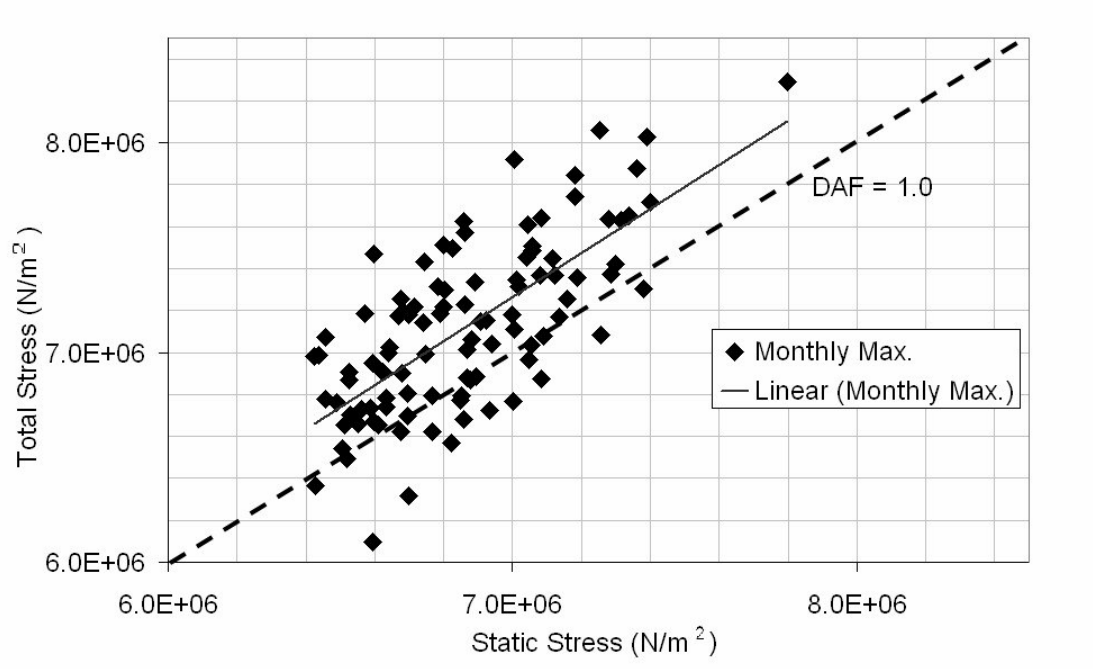

Figure 8 Correlation between maximum static and total stress.

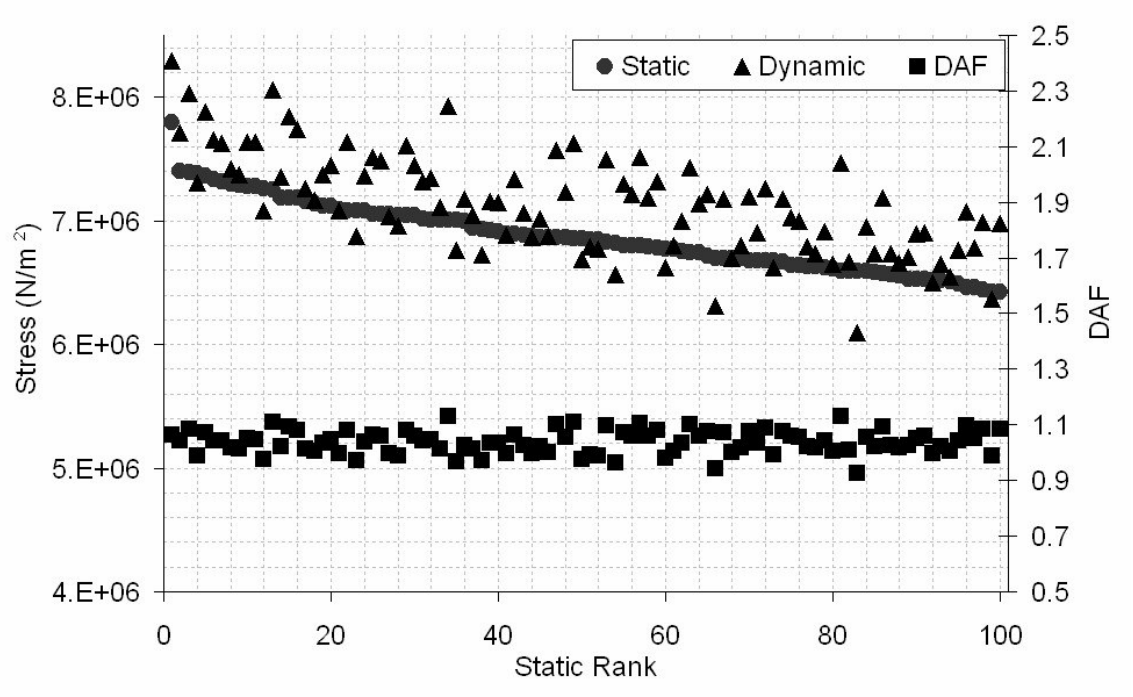

Figure 9 Ranking of events by maximum static response.